

Online supplementary material to Buckled Diamond-like Carbon Nanomechanical Resonators

M. Tomi,¹ A. Isacson,² M. Oksanen,¹ D. Lyashenko,¹ J.-P. Kaikkonen,¹ S. Tervakangas,³ J. Kolehmainen,³ and P. J. Hakonen¹

¹Low Temperature Laboratory, Department of Applied Physics, Aalto University, P.O. Box 15100, FI-00076 AALTO, Finland.

²Department of Applied Physics, Chalmers University of Technology, SE-412 96 Göteborg, Sweden.

³DIARC-Technology Oy, Kattilalaaksontie 1, FI-02330 Espoo, Finland.

(Dated: 7 August 2015)

These supplementary notes to the paper Buckled Diamond-like Carbon Nanomechanical Resonators are organized as follows: First, we present and discuss some details of our measurement data for the diamond-like carbon (DLC) resonators. This is followed by a section where we highlight the importance of a good mechanical contact between DLC and the support structure; a feature that we believe is the origin of the smallness of the measured effective resonator width W . We then present measurements on surface roughness and discuss its relation to the material parameters used to fit the measured data to the model. We end by giving a detailed account for the derivation of the equations describing the eigenspectrum of buckled beams under electrostatic load.

TRANSMISSION OF THE MOTIONAL BRANCH

Transmission through the DLC resonator device was measured with a vector network analyzer (VNA), which enabled recording both magnitude and phase information. As the impedance of the parasitic capacitance is smaller than the impedance of the motional RLC resonator, the resonance lineshape consists of an upward peak, followed immediately by a downward peak. If we subtract the vector background that arises due to parasitics, we are left with a transmission spectrum for the motional RLC branch only (Fig. 1a). The magnitude of this motional RLC resonance takes on the conventional Lorentzian lineshape, limited by noise from the VNA when moving far away from resonance.

To visualize the complex form of the transmission, we can plot its real and imaginary parts in the complex plane while sweeping frequency near the resonance (Fig. 1b). This representation, known as the Nyquist plot, should form a circular or an elliptical response depending on whether the resonance is linear or nonlinear, respectively. From Fig. 1b we can deduce that no prominent nonlinear effects are present in the DLC resonator at low drive powers.

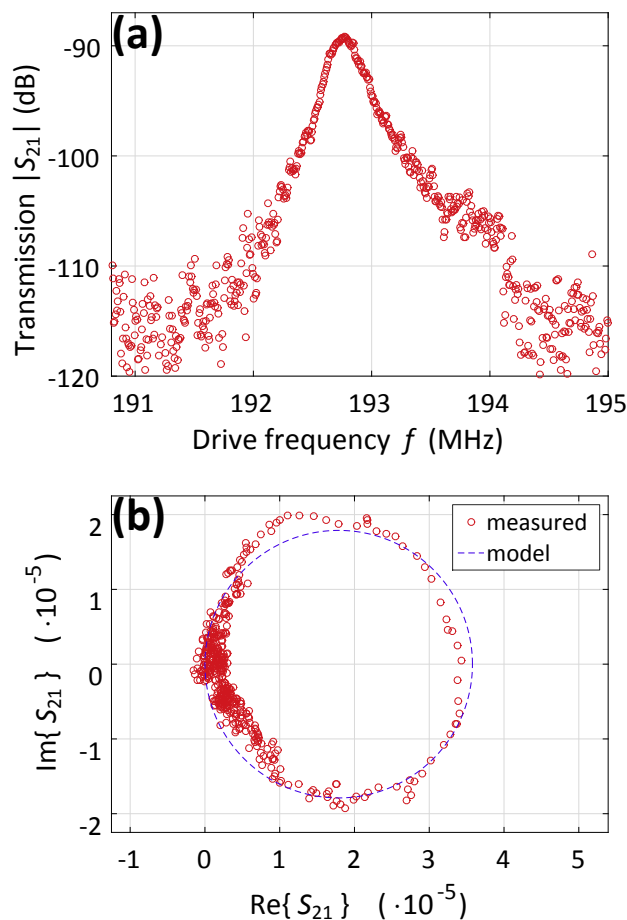


FIG. 1. (a) Transmission through the DLC resonator at dc bias $V_{dc} = -10$ V and $P = -40$ dBm with parasitic components subtracted. (b) Nyquist plot of the same data in the complex plane. The dashed blue line shows a circular fit given by the (motional) RLC model.

IMPERFECT BOUNDARY CONDITIONS

In our measurements we have found that sometimes the boundary conditions of the resonator are not well defined. This is because of the weak adhesion of DLC to the supporting Au electrodes. The compressive stress in the DLC film may partially detach it from the Au surface,

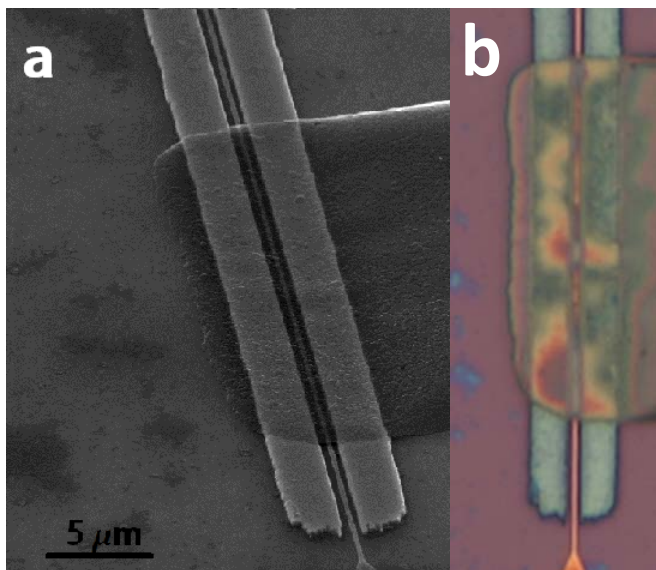


FIG. 2. (a) SEM image of a DLC resonator with imperfect boundary conditions. (b) Optical image of the device, which shows the irregularities in the clamping. The irregularities split the uniform oscillations into several separate modes. This reduces the width W of the resonating region.

which leads to ambiguous boundary conditions. These, in turn, lead to the localization of the resonance modes. Fig. 2 shows scanning electron microscope (SEM) and optical images of one particular device with very poor attachment, and where several resonances were detected. The effect of the imperfect boundary conditions is thus that the actual width W of the vibrating region can be considerably smaller than the width of the entire DLC sheet. Also, in the better-contacted devices, small irregularities in the clamping can be sufficient to cause splitting of the modes.

FITTING OF THE FREQUENCY TUNING AND SURFACE ROUGHNESS

While some of the device parameters are known to good accuracy, others, such as the thickness t , are harder to quantify precisely. For nanoresonators it is known that the effective elastic properties change as the surface-to-volume ratio increases⁴. Hence, for a resonator made of a material with Young's modulus E , an effective modulus $E^* \neq E$ may be needed.

The DLC films used here nominally have a thickness of $t \approx 20$ nm, measured using a DektakXT profilometer. However, the degree of surface roughness arising from the fabrication process is relatively large, with a full width at half maximum (FWHM) on the order of 10 nm as characterized by atomic force microscope (AFM) measurements (see Fig. 3). This suggests that the dominating surface effects in our case stem from the surface roughness.

A common model for including the effect of the sur-

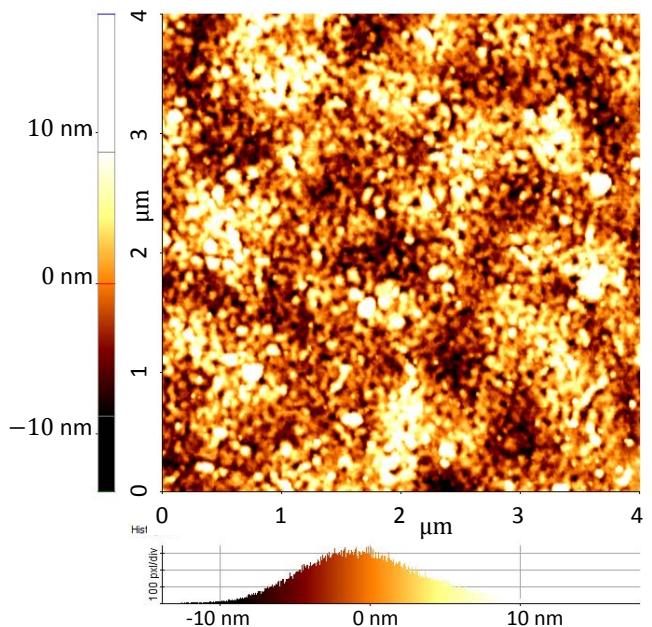


FIG. 3. (top) False colour AFM image of the DLC film. (bottom) Histogram over the surface height distribution.

face is to treat the body as a perfect solid, and emulate the surface effects by enclosing it in a 2D elastic membrane⁵. Following this approach, it has been shown that surface roughness leads to a membrane enclosure which can have a negative effective Young's modulus⁶. For resonator structures, it was further shown that this decreases the resonant frequency in comparison to using the bulk value. As a result, the Young's modulus can be replaced by an effective one with a value below the bulk value.

While we have chosen to use the thickness as measured by the profilometer, *i.e.* $t = 20$ nm, when fitting the frequency tuning, it is also possible to fit the data assuming larger thicknesses, up to $t \approx 25$ nm. However, increasing the thickness requires using a higher effective Young's modulus to fit the measured data. From indentation measurements, we have an upper bound $E \leq 180$ GPa which in practice limits the thickness that can be used in the fitting.

MECHANICAL MODEL AND RESONANT RESPONSE

This section details the mathematical procedure for finding the resonant frequencies of the Euler-buckled beam subject to an external (electrostatic) load. The fitting of the frequency tuning curves, including both geometric and electrostatic nonlinearities, were done by numerically solving the resulting equations for the stationary problem [Eqs. (3) and (5)] and then for the eigenfrequencies [Eq. (6)].

To obtain the necessary equations, we model the sus-

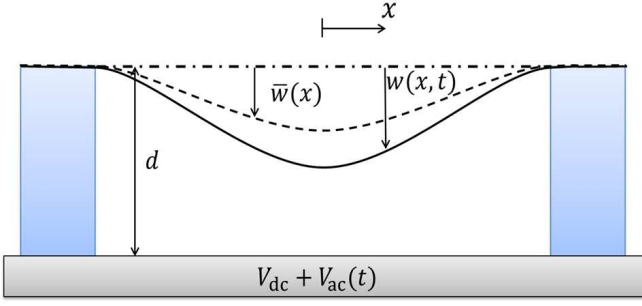


FIG. 4. Schematic sideview of a downward buckled DLC membrane of length L , downward deflection $w(x, t) = \bar{w}(x) + \delta w(x, t)$ subject to a bias voltage $V(t) = V_{dc} + V_{ac}(t)$.

pendent part of the DLC resonator as a wide uniform plate with the material parameters shown in Table I. This makes the system essentially a 1D problem, namely that of the vibrations of a buckled beam as shown in Fig. 4.

For a bias voltage $V(t) = V_{dc} + V_{ac}(t)$, the equation of motion using the Euler–Bernoulli beam theory is in the parallel-plate approximation²

$$\begin{aligned} \rho h W \partial_t^2 w + \frac{E W h^3}{12} \partial_x^4 w - \sigma W h \partial_x^2 w &= \frac{\epsilon_0 V^2 W}{2(d-w)^2}, \\ \sigma &= \sigma_0 + \frac{E W h}{2L} \int_{-L/2}^{L/2} dx (\partial_x w)^2, \\ w(\pm L/2) = \partial_x w(\pm L/2) &= 0, \end{aligned} \quad (1)$$

where the small correction due to a finite Poisson's ratio ν has been neglected. Rescaling Eq. (1), *i.e.*, putting it on dimensionless form with characteristic length scale L and timescale $(12\rho L^4/Eh^2)^{1/2}$ gives the system of equations

$$\begin{aligned} [\partial_\tau^2 + \partial_x^4 - T \partial_x^2] w &= f, \\ T &= -T_0 + \alpha \int_{-1/2}^{1/2} dx (\partial_x w)^2, \\ w(\pm 1/2) = \partial_x w(\pm 1/2) &= 0. \end{aligned} \quad (2)$$

Here, $T = 12\sigma L^2/Eh^2$, $T_0 = -12\sigma_0 L^2/Eh^2$, $f \approx f_0/[1 - \frac{w}{d}]^2$, with $f_0 = 6\epsilon_0 L^3 V_{dc}^2/d^2 E h^3$ and $\alpha = 6L^2/h^2$.

Static solution

To find the response of the sheet we first seek the static solution. Hence, we set $w = \bar{w}(x) + \delta w(x, t)$ and consider the static problem $[\partial_x^4 - T \partial_x^2] \bar{w} = f_0(1 - \bar{w}/d)^{-2} = \bar{f}$, with $T = -T_0 + \alpha \int dx (\partial_x \bar{w})^2$.

Depending on the sign of the resulting static tension \bar{T} one finds the solutions

$$\bar{w}_- = -\frac{\bar{f}}{2\bar{T}} \left(x^2 - \frac{1}{4} \right)$$

TABLE I. Parameters and quantities used in the modeling of the DLC membrane resonator.

Quantity/parameter	Symbol	Value or range
Width,	W	
Length	L	1 μm
Thickness	h	20 nm (<25 nm)
Mass density	ρ	2000 kg/m ³
Young's modulus	E	140 GPa to 180 GPa
Suspension height	d	205 nm
Bias voltage	$V(t)$	
In-plane stress	$\sigma(t)$	
Initial compressive stress	$-\sigma_0$	<2.0 GPa
Vacuum permittivity	ϵ_0	8.854×10^{-12} F/m
Vertical deflection	$w(x, t)$	$(-\frac{L}{2} < x < \frac{L}{2})$

$$+ \frac{\bar{f}}{2|\bar{T}|^{3/2}} \frac{\cos\left(\sqrt{|\bar{T}|}x\right) - \cos\left(\frac{1}{2}\sqrt{|\bar{T}|}\right)}{\sin\left(\frac{1}{2}\sqrt{|\bar{T}|}\right)} \quad (3)$$

for $\bar{T} < 0$ and

$$\begin{aligned} \bar{w}_+ &= -\frac{\bar{f}}{2\bar{T}} \left(x^2 - \frac{1}{4} \right) \\ &+ \frac{\bar{f}}{2|\bar{T}|^{3/2}} \frac{\cosh\left(\sqrt{|\bar{T}|}x\right) - \cosh\left(\frac{1}{2}\sqrt{|\bar{T}|}\right)}{\sinh\left(\frac{1}{2}\sqrt{|\bar{T}|}\right)} \end{aligned} \quad (4)$$

for $\bar{T} > 0$. The equilibrium tension is found from solving the equations

$$\bar{T} = -T_0 + \alpha \frac{\bar{f}^2}{\bar{T}^2} \left(\frac{2}{\bar{T}} + \frac{1}{12} + \frac{1}{8\sqrt{|\bar{T}|}} \frac{\sqrt{|\bar{T}|} + 3\sin\sqrt{|\bar{T}|}}{\sin^2 \frac{1}{2}\sqrt{|\bar{T}|}} \right) \quad (5)$$

for $\bar{T} < 0$ and

$$\bar{T} = -T_0 + \alpha \frac{\bar{f}^2}{\bar{T}^2} \left(\frac{2}{\bar{T}} + \frac{1}{12} - \frac{1}{8\sqrt{\bar{T}}} \frac{\sqrt{\bar{T}} + 3\sinh\sqrt{\bar{T}}}{\sinh^2 \frac{1}{2}\sqrt{\bar{T}}} \right), \quad \bar{T} > 0.$$

Note that although Eq. (3) seems to give zero static deflection when $\bar{f} \rightarrow 0$, the Euler buckling solutions for $\bar{f} = 0$ are contained in the solution Eq. (3) due to the limiting behavior of Eq. (5) when $f \rightarrow 0$.

Small vibrations around equilibrium

To find the resonant mode shape and frequency of the fundamental mode, we linearize Eq. (2) around the equilibrium solution \bar{w} to obtain the eigenvalue problem

$$\left[\partial_t^2 + \partial_x^4 - \bar{T} \partial_x^2 - \frac{2\bar{f}}{d - \bar{w}} \right] \delta w = \delta T \partial_x^2 \bar{w},$$

where $\delta T = 2\alpha \int dx (\partial_x \bar{w}) (\partial_x \delta w) = -2\alpha \int dx \delta w \partial_x^2 \bar{w}$. This eigenvalue problem has the general form

$$(\partial_x^4 - T\partial_x^2 - \lambda^2)u = -h(x) \int dx' h(x')u(x')$$

with $\lambda^2 = \omega^2 + 2\bar{f}/(d - \bar{w})$ and

$$h(x) = \begin{cases} \sqrt{2\alpha} \frac{\bar{f}}{|\bar{T}|} \left(1 - \frac{\sqrt{|\bar{T}|}}{2} \frac{\cos \sqrt{|\bar{T}|}x}{\sin \frac{1}{2}\sqrt{|\bar{T}|}} \right), & \bar{T} < 0 \\ \sqrt{2\alpha} \frac{\bar{f}}{|\bar{T}|} \left(-1 + \frac{\sqrt{|\bar{T}|}}{2} \frac{\cosh \sqrt{|\bar{T}|}x}{\sinh \frac{1}{2}\sqrt{|\bar{T}|}} \right), & \bar{T} > 0. \end{cases}$$

Following Ref.³ we set $u = u_0 + Ah(x)$ and note that $(\partial_x^4 - \bar{T}\partial_x^2)h(x) = 0$. This implies that the solution to the problem is found by solving the simultaneous equations

$$(\partial_x^4 - \bar{T}\partial_x^2 - \lambda^2)u_0 = 0, \quad A\lambda^2 = \int dx h(x) [u_0(x) + Ah(x)].$$

Below we will restrict attention to the fundamental mode examined in the main part of the paper.

Fundamental mode resonant frequency, compressive stress

For $\bar{T} < 0$ we make the following Ansatz for the fundamental mode

$$u_0 = B\cos \beta x + C\cosh \gamma x$$

leading to the secular equations $\beta^4 - |\bar{T}|\beta^2 - \lambda^2 = 0$ and $\gamma^4 + |\bar{T}|\gamma^2 - \lambda^2 = 0$. To satisfy the boundary conditions one must further fulfill the relations

$$Ah(1/2) + B\cos \beta/2 + C\cosh \gamma/2 = 0$$

$$Ah'(1/2) - B\beta\sin \beta/2 + C\gamma\sinh \gamma/2 = 0.$$

As we are only interested in the spectrum, we are free to choose the normalization such that $A = 1$. Hence,

to find the frequency of the fundamental mode under compressive stress one should solve the equation

$$\lambda^2 = \int dx h(x) [B\cos(\beta x) + C\cosh \gamma x + h(x)]. \quad (6)$$

Here β, γ, B and C depend on λ^2 according to

$$\beta = \sqrt{\sqrt{\bar{T}^2/4 + \lambda^2} - \bar{T}/2}, \quad \gamma = \sqrt{\sqrt{\bar{T}^2/4 + \lambda^2} + \bar{T}/2}, \quad (7)$$

$$B = -\frac{\gamma h(1/2) \sinh \gamma/2 - h'(1/2) \cosh \gamma/2}{\beta \cosh \gamma/2 \sin \beta/2 + \gamma \sinh \gamma/2 \cos \beta/2}, \quad (8)$$

$$C = -\frac{\beta h(1/2) \sin \beta/2 + h'(1/2) \cos \beta/2}{\beta \cosh \gamma/2 \sin \beta/2 + \gamma \sinh \gamma/2 \cos \beta/2}. \quad (9)$$

The mode shapes and resonant frequencies can now be found by solving the eigenvalue equation [Eq. (6)] for λ^2 . While some progress can be made analytically by carrying out the integrals, a numerical solution is needed to find the spectrum.

Fundamental mode, tensile stress

For completeness we also briefly comment on the solution for tensile stress $\bar{T} > 0$. In this case the same Ansatz can be used for the fundamental mode shape, *i.e.*, $u_0 = B\cos \beta x + C\cosh \gamma x$. However, the equations for wavenumbers become reversed, and we now get $\beta^4 + |\bar{T}|\beta^2 - \lambda^2 = 0$ and $\gamma^4 - |\bar{T}|\gamma^2 - \lambda^2 = 0$. The formulas for coefficients B and C remain unchanged.

REFERENCES

- ¹X. Song, M. Oksanen, M. A. Sillanpää, H. Craighead, J. Parpia, and P. J. Hakonen, *Nano Lett.* **12**, 198 (2011).
- ²K. F. Graff, *Wave Motion in Elastic Solids*, Oxford University Press 1975, Toronto.
- ³A. H. Nayfeh and S. A. Emam, *Nonlinear Dynam.* **54**, 395 (2008).
- ⁴K. B. Gavan, H. J. R. Westra, E. W. J. M. van der Drift, W. J. Venstra, and H. S. J. van der Zant, *Appl. Phys. Lett.* **94**, 233108 (2009).
- ⁵M. E. Gurtin and A. I. Murdoch, *Arch. Ration. Mech. An.* **57**, 291 (1975).
- ⁶P. Mohammadi, L. P. Liu, P. Sharma, and R. V. Kukta, *J. Mech. Phys. Solids* **61**, 325 (2013).